Hybrid Hall effect device

Mark Johnson,[a] Brian R. Bennett, M. J. Yang, M. M. Miller, and B. V. Shanabrook
Naval Research Laboratory, Washington, D.C. 20375

(Received 6 February 1997; accepted for publication 16 June 1997)

A novel magnetoelectronic device incorporating a single microstructured ferromagnetic film and a micron scale Hall cross was fabricated and characterized at room temperature. Magnetic fringe fields from the edge of the ferromagnet generate a Hall voltage in a thin film semiconducting Hall bar. The sign of the fringe field, as well as the sign of the output Hall voltage, is switched by reversing the magnetization of the ferromagnet. This new device has excellent output characteristics and scaling properties, and may find application as a magnetic field sensor, nonvolatile storage cell, or logic gate. © *1997 American Institute of Physics.* [S0003-6951(97)01133-9]

In the emerging field of magnetoelectronics, the most common devices are based on giant magnetoresistance[1] or on spin polarized tunneling,[2] and share a common trait: output is characterized as a resistance that varies between two positive values, R and $R+\delta R$. A third device, the bipolar spin transistor,[3] is characterized by a bipolar output, $\pm\delta R$. The advantage of a bipolar output is increased utility. For example, the output of one device may be used to control the magnetic state of a second device,[4] and positive (negative) currents be used to set a positive (negative) magnetization state. Furthermore, an offset can be conveniently added to the output resulting in values of zero (or LOW) and HIGH, values that are more useful than V and $V+\delta V$. The devices listed above all rely on the transport of spin polarized current in structures comprised of multilayers of ferromagnetic and nonmagnetic metals. By contrast, this letter introduces a novel magnetoelectronic device that uses a single electrically isolated ferromagnetic (F) layer, does not depend on spin polarized transport, and has a bipolar output of order $\pm 10\Omega$ or more. Large magnetic fringe fields at the edge of a ferromagnetic film fabricated above a microstructured Hall cross cause a Hall effect on the carriers of a high mobility semiconductor (S) and generate the bipolar output.[5] The magnetic fringe field has a magnitude that is large at the edge of the F film, and decays rapidly with increasing distance from the edge. We demonstrate micron scale devices with an output characterized by LOW$<1\Omega$, and a ratio of HIGH/LOW$\approx$25.

The device is depicted schematically with a top view in Fig. 1(a). The Hall bar is fabricated from a high mobility indium arsenide film, described below, and is current biased from left to right through arms of width w_I. The sense probes $S1$ and $S2$ have width w_V and may be fabricated, for reasons described below, with a small asymmetry x_0. Typical dimensions of w_I and w_V are a few microns, and x_0 is the order of 100 nm or less. In the devices described herein, F is a thin film transition metal ferromagnet with thickness $d_f\approx 150$ nm and in-plane magnetization **M**. Typical dimensions of each edge of F are w_I+2 μm, and F is located with one edge at distance x_f from the center of the Hall cross.

As seen in the cross-sectional view of Fig. 1(b) (not drawn to scale), the heterostructure is grown by molecular beam epitaxy and consists of: 3 nm InAs/3 nm GaSb/25 nm AlSb/15 nm InAs/2 μm AlSb [I_2 in Fig. 1(b)]/semi-insulating GaAs (001) substrate. After the Hall cross is fabricated by photolithography and a standard mesa etch, a 45 nm layer of SiO is deposited over the chip to passivate the AlSb. The F layer is fabricated by photolithography and lift-

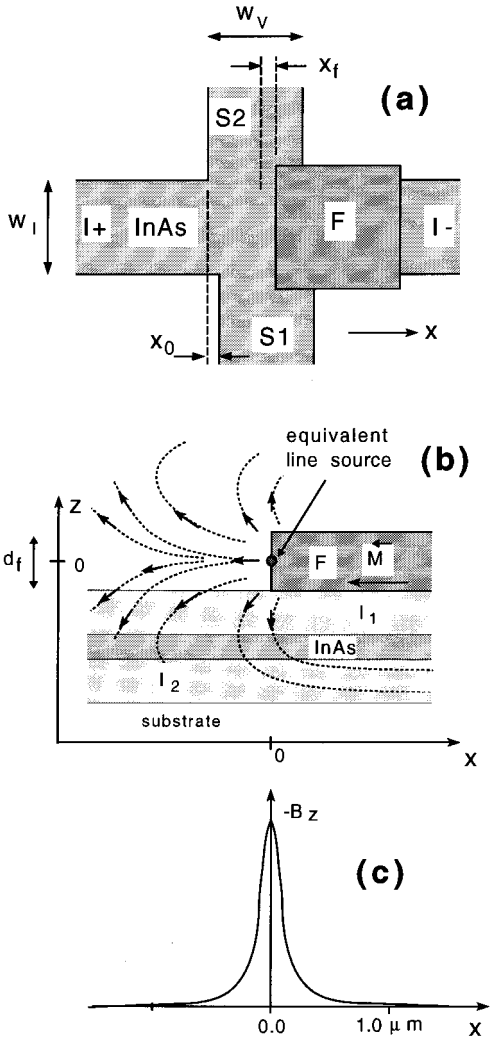

FIG. 1. Schematic diagram of the device geometry. (a) Top view; (b) cross-section view, showing fringe field near the edge of F; and (c) profile of the spatial dependence of the perpendicular component B_z as calculated from a line charge model.

[a]Electronic mail: mjbooj@anvil.nrl.navy.mil

 0003-6951/97/71(7)/974/3/$10.00

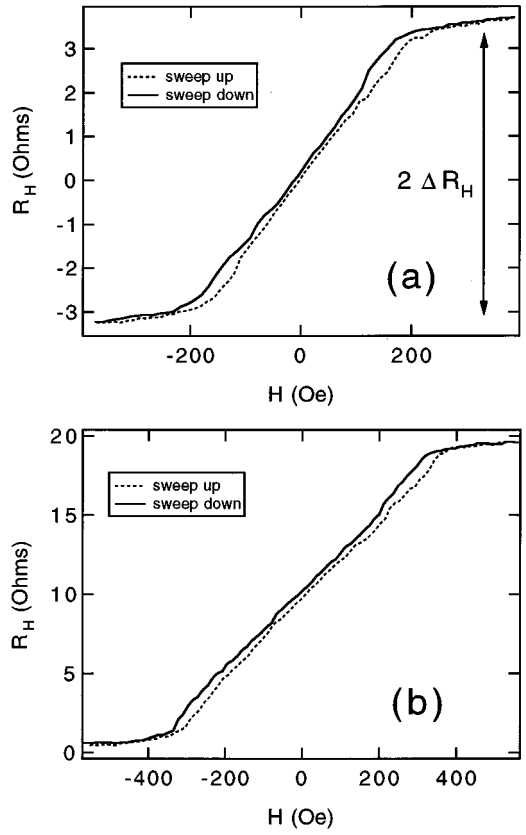

FIG. 2. Typical data, R_H vs H at 295 K. (a) Device HB1AA-II, $w_I = 5\ \mu$m, $W_V = 3\ \mu$m. (b) Device HB1A-VIII, $w_I = 2\ \mu$m, $W_V = 1\ \mu$m.

off, and F is electrically isolated from S by the insulating layer I_1 of total thickness 76 nm.

The principle of device operation can be readily explained with the aid of Fig. 1. When the magnetization **M** of F is saturated along $-\hat{x}$, positive magnetic ''poles'' at the edge of F generate an external field **B**, depicted in Fig. 1(b) by arrows and dashed field lines. A large negative component $-B_z$, perpendicular to the plane of S, generates a negative Hall voltage from $S1$ to $S2$. When an external in-plane field H reverses the magnetization, the perpendicular component of fringe field B_z also changes sign resulting in a positive Hall voltage from $S1$ to $S2$. Thus, the ferromagnetic film performs as a magnetic field transducer acting on a local region of S and changing a small magnetic field $H\hat{x}$ into a larger field substantially perpendicular to the plane.

When the Hall cross is fabricated with perfect symmetry [$x_0 = 0$ in Fig. 1(a)], the output of the hybrid Hall device has symmetrically bipolar values $\pm R_H$ as H is swept from positive to negative, reversing the magnetization **M** of F. A small asymmetry in fabrication of sense probes $S1$ and $S2$ [$x_0 \neq 0$ in Fig. 1(a)] results in the series addition of a small offset resistance R_o to the output measured from $S1$ to $S2$. We demonstrate this with devices having minimal offset resistance, $|R_H|/R_o \approx 30$ [Fig. 2(a)]. If the offset resistance equals the magnitude $|R_H|$, the baseline resistance R_b equals zero, and the hybrid Hall device output has levels zero (or LOW) and HIGH. We demonstrate this with devices having R_b near zero, $|R_H|/R_b \approx 25$ [Fig. 2(b)].

The indium arsenide film had a room temperature density of $n = 1.8 \times 10^{12}$ cm^{-2} (Hall sensitivity of 347Ω/tesla), mobility of 20 000 V/cm^2, and sheet resistance of $R_\square = 170\Omega/\square$. The F film was Permalloy, e-beam deposited from a charge of $Ni_{0.8}Fe_{0.2}$ at a pressure of 4×10^{-6} Torr. Characterization by SQUID magnetometry of a witness film deposited on a quartz substrate (about 0.09 cm^2), alongside the sample chip showed a room temperature saturation magnetization of 860 ± 20 emu/cm^3, a square hysteresis loop, and a coercivity of $H_c = 3$ Oe.

Transport measurements on the hybrid Hall devices were performed at room temperature using an audio frequency bias source, and a lock-in amplifier. The detected Hall voltage was linear with bias current for the current range of 0.01–3 mA, and is presented as a resistance R_H.

Typical data from two devices are presented in Fig. 2. The symmetrically bipolar output of Fig. 2(a) is from a device with $R_o \approx 0$ ($x_0 \approx 0$). The data in Fig. 2(b) are from a device with $R_o \approx |R_H|$ ($x_0 \sim 100$ nm). In all, data were taken on device sets with dimensions (w_I, w_V) of (5 μm, 3 μm), (3 μm, 2 μm) and (2 μm, 1 μm).

When $R_0 = 0$, the $R_H - H$ traces are essentially the same as the $M - H$ loop of the ferromagnet F, with $R_H \propto M$. In Fig. 2(a), R_H varies linearly with H for low fields, saturates at a coercive field of about ± 200 Oe, and the loop shows low hysteresis and small remanance. In our device sets H_c increased as the dimensions of F decreased [compare Figs. 2(a) and 2(b)]. As is commonly observed in patterned films, this behavior of $R_H(H)$, and equivalently of $M(H)$, is different from the classic loop of the macroscopic witness film and is due to micromagnetism. The larger coercivity is caused by demagnetizing fields, which are dominant in microstructured films with dimensions of order 1 μm. Our coercivities of order 100 Oe for 3–7 μm square films, and the observed trend of increasing coercive values for smaller film dimensions, are in good agreement with other reports.[6,7]

The low remanance is a result of a ''degenerate'' picture frame domain pattern that minimizes free energy, and yields zero pole density at the edge of F in zero applied field. Figure 3 is a MFM image (phase channel, tapping mode) of a 7 μm by 7 μm Permalloy film in zero external field. A micron wide area at the perimeter has no magnetization information because of tip perturbations at ''rough'' film edges (caused by artifacts of processing), but the central closed domain pattern that we observe confirms the zero magnetization state that we deduce from our measurement of $R_H(H = 0)$. As H increases along $\hat{x}$, the domain aligned with **H** increases as the domain wall moves along $\hat{y}$, and the pole density at the edge of F increases linearly. Field sweeps over a range $|H| = 150$ Oe showed good linearity of $R_H(H)$ and no remanence, indicating that the domain wall moves back and forth elastically in this field range.

Quantitatively, the magnitude of R_H measured in our prototype devices can be compared with an estimate based on a semiquantitative magnetostatic calculation. When saturated, F is assumed to be a single domain with $\mathbf{M} = M_s\hat{x}$. The fringe field **B** is generated by magnetic ''poles'' with magnetic surface charge density M_s (magnetic ''charge'' per unit area) at the edge of F. In a simplified calculation, M_s is approximated as a concentration of poles on a line along the edge of F, a distance $d_f/2$ above the surface of I_1 [Fig. 1(b)], where d_f is the thickness of F. For an infinite line of mag-

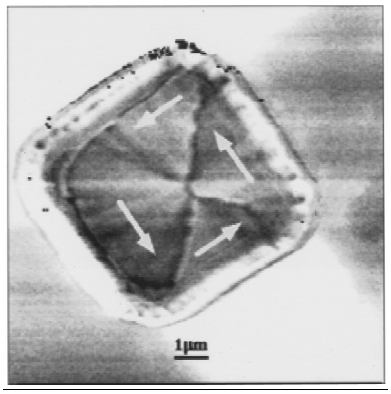

FIG. 3. MFM image of a 7 μm by 7 μm Permalloy F film in zero applied field. Arrows indicate the closure pattern of the four domains.

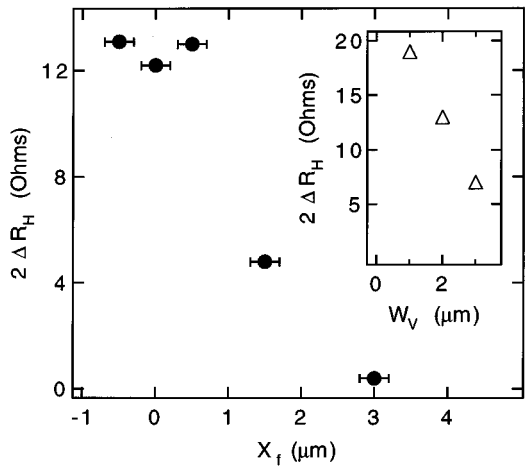

FIG. 4. $2\Delta R_H$ vs x_f for a family of devices with $w_I=3$ μm, $w_V=2$ μm. Inset: $2\Delta R_H$ vs w_V.

netic charge density $\lambda_m=M_s d$, the radial field has magnitude at radius r given by $B_r(r)=2\lambda_m/r$. The fringe field from the other edge of F is neglected, as justified by the results below. At the plane of the InAs layer this yields $B_z(x)=2\lambda_m R/(x^2+R^2)$, where x is the lateral distance between the edge of F and the point r, and $R=155$ nm is the depth of the InAs layer relative to λ_m. For our samples we have $M_s\approx 860\pm 20$ emu/cm^3 and $d_f=150\pm 10$ nm. The profile of the magnitude of B_z is sketched in Fig. 1(c). The peak value, at $x=0$, is $B_z\approx 1650$ Oe and the magnitude falls rapidly to $B_z\approx 100$ at $x=0.5$ μm.

The Hall voltage developed in the cross junction is given by the line integral of the cross product of B_z and the bias current. Traditionally, the magnetic field is constant and the integration is straightforward. In our novel devices the field has a gradient $\partial B_z/\partial x$ that is steep on the scale of the width W_V of the cross and transport is more complicated. A *crude* estimate of the expected magnitude of R_H can be made by simply averaging $B_z(r)$ along x, over a distance corresponding to the width W_V of the sense probes $S1$ and $S2$.

We define ΔR_H to be the value of R_H for saturation magnetization [Fig. 2(a)]. The full bipolar resistance swing upon magnetization reversal is approximately given as $2\Delta R_H\approx 2\langle B_z\rangle/(n_s e)$, where $\langle B_z\rangle$ is the average perpendicular field. The magnitude $2\Delta R_H$ is plotted as a function of x for a family of devices in Fig. 4. The amplitude $2\Delta R_H$ decays rapidly with increasing x as expected, and we note that the Hall cross has lithographically rounded edges that act to broaden the decay. The peak magnitude of 13.1Ω corresponds to an average field of 190 Oe, somewhat less than the value $B_z=360$ calculated from the model presented above, but in reasonable agreement considering the simplicity of the model. The datum point at $x=3.0$ μm represents a control sample: a F film with dimensions 5 μm by 8 μm is centered over the Hall cross; so that each edge is 2 μm away from any region of the sense probes, and $\Delta R_H\rightarrow 0$ as expected.

Since $\langle B_z\rangle$ is ''averaged'' over the width w_V, the amplitude $2\Delta R_H$ is expected to increase for decreasing w_V and the hybrid Hall device is characterized by inverse scalability: the output characteristic improves as the dimensions of the device are shrunk. The inset of Fig. 4 plots the peak magnitude $2\Delta R_H$ as a function of sense probe width w_V. The linear decrease of $2\Delta R_H$ demonstrates inverse scalability and confirms the simple model presented above.

The devices presented herein demonstrate a linear field response over a large region of field, have low remanence and large output, and therefore, are well suited for application as a field sensor. When fabricated with a ferromagnetic material with large anisotropy and large intrinsic remanence,[8] the hybrid Hall device is ideally suited for application as a nonvolatile memory cell or a single element logic gate.[4] Furthermore, device fabrication is relatively simple, requiring only two lithographic steps. High mobility indium arsenide is an excellent material choice for the Hall bar, but good devices can be made from any material with a reasonable Hall coefficient. Finally, following the recent demonstration of nm scale semiconducting ''wires'' [9] and nm scale single domain ferromagnetic particles,[10] the hybrid Hall device offers a novel mechanism for the fabrication of nm scale devices with bipolar output.

The authors are grateful to B. Nadgorny, R. J. Wagner, and J. B. Boos for technical assistance. This work was supported by the Office of Naval Research.

[1] For a recent review, see G. A. Prinz, Phys. Today **48**, 58 (1995).
[2] J. S. Moodera, L. R. Kinder, T. M. Wong, and R. Meservey, Phys. Rev. Lett. **74**, 3273 (1995).
[3] M. Johnson, Phys. Rev. Lett. **70**, 2142 (1993).
[4] M. Johnson, IEEE Spectr. **31**, 47 (1994).
[5] For a review of Hall devices, see R. S. Popovic, *Hall Effect Devices* (Adam Hilger, Bristol, 1991).
[6] J.-G. Zhu, Y. Zheng, and X. Lin, J. Appl. Phys. **81**, 4336 (1997).
[7] G. A. Gibson and S. Schultz, J. Appl. Phys. **73**, 4516 (1993).
[8] A set of devices has been fabricated with cobalt and demonstrates good remanance and voltage output levels>50 mV. M. Johnson (unpublished).
[9] C. W. Beenaker and H. Van Houten, Solid State Phys. **44**, 1 (1991).
[10] D. D. Awschalom and D. P. DiVincenzo, Phys. Today **48**, 58 (1995).